

# UNSTEADY FRICTION CHARACTERISTIC OF HYDRAULIC ACTUATOR AND ITS MATHEMATICAL MODEL

Hideki YANADA\*, Yuta SEKIKAWA\*\*, Kazuya TAKAHASHI\*\*\* and Akinori MATSUI\*\*\*\*

\* Department of Mechanical Engineering, Toyohashi University of Technology  
1-1 Hibarigaoka, Tempaku-cho, Toyohashi, 441-8580 Japan  
(E-mail: yanada@mech.tut.ac.jp)

\*\* Fanuc Ltd. Oshino-mura, 401-0597 Japan

\*\*\* Sony Energy Devices Corporation

1-1 Shimosugishita, Takakura, Hiwada-machi, Koriyama, 963-0531 Japan

\*\*\*\* Graduate student, Department of Mechanical Engineering,  
Toyohashi University of Technology

## ABSTRACT

This paper deals with unsteady-state friction characteristics of a hydraulic actuator. Using a single rod hydraulic cylinder, friction characteristics are experimentally investigated under various conditions of velocity variation at different supply pressures. The friction force of the hydraulic cylinder is measured based on the equation of motion using measured values of the pressures in the cylinder chambers and the acceleration of the hydraulic piston. A method to identify dynamic parameters included in the modified LuGre model, which has been proposed by Yanada and Sekikawa, is proposed. Comparison between measured unsteady-state friction characteristics and those simulated by the modified LuGre model is conducted. It is shown that the unsteady-state friction characteristics simulated using the parameters identified agree with those obtained by experiments with a relatively good accuracy and that the proposed method to identify the dynamic parameters is appropriate. The effect of the supply pressure on the friction characteristics and the dynamic parameters are shown.

## KEY WORDS

Hydraulic actuator, Unsteady friction, Mathematical model, Modified LuGre model, Parameter identification

## NOMENCLATURE

$A_i$  : piston area ( $i=1,2$ )

$a$  : acceleration

$F_c$  : Coulomb friction force

$F_r$  : friction force

$F_{rss}$  : steady-state friction force

$F_s$  : maximum static friction force

$\mathbf{f}$  : observer gain vector

$g$  : Stribeck function

$h$  : dimensionless unsteady-state lubricant film thickness

$h_{ss}$	: dimensionless steady-state lubricant film thickness
$K_f$	: proportional constant for lubricant film thickness
$m$	: load mass
$n$	: exponent for Stribeck curve
$p_i$	: pressure ( $i=1,2$ )
$p_s$	: supply pressure
$t$	: time
$t_d$	: dwell time
$u$	: control input (servo current)
$v$	: velocity
$v_b$	: upper (for $v>0$ ) or lower (for $v<0$ ) limit of velocity range where $h_{ss}$ or $h$ is varied
$v_s$	: Stribeck velocity
$x_p$	: piston position
$z$	: mean deflection of bristles
$\sigma_0$	: stiffness of bristles
$\sigma_1$	: micro-viscous friction coefficient for bristles
$\sigma_2$	: viscous friction coefficient
$\tau_h$	: time constant for lubricant film dynamics
$\tau_{hp}$	: time constant for acceleration period
$\tau_{hm}$	: time constant for deceleration period
$\tau_{h0}$	: time constant for dwell period

## INTRODUCTION

Accurate modeling of static and dynamic characteristics of each fluid power component is very important to analyze the performance and/or dynamics of or to predict the behaviors of a fluid power system. Friction is always present in fluid power components having sliding parts and especially that of a fluid power actuator may have some undesirable influence on the performance of a fluid power system. Mathematical models to describe the steady-state friction characteristics have been proposed [1-3] and are widely used to analyze the steady-state characteristics of a fluid power actuator. However, those models are useless to predict dynamic behaviors of the actuator especially when the actuator repeats start/stop.

The unsteady-state friction characteristics of a hydraulic motor has been examined by Yanada et al. [4] by varying the rotational speed sinusoidally in one direction in the negative resistance regime. It has been shown that the friction torque traces the steady-state friction torque-velocity curve, i.e., the Stribeck curve, at very low frequencies of the velocity variation, that the negative slope of the friction torque-velocity curve is decreased as the frequency of the velocity variation is increased, and that the negative slope becomes almost null at relatively high frequencies.

Several mathematical models that describe the dynamic behaviors of friction have been proposed [5-9] and among them, the LuGre model [6] is most widely utilized. However, all the models proposed so far cannot simulate well the friction behaviors of a hydraulic motor

in the sliding regime shown in [4]. Yanada and Sekikawa have made a modification to the LuGre model by incorporating lubricant film dynamics into the model and have shown that the proposed model, called the modified LuGre model, can simulate dynamic behaviors of friction observed with a hydraulic cylinder with a relatively good accuracy [10].

However, the dynamic parameters,  $\sigma_0$ ,  $\sigma_1$ ,  $\tau_h$ , included in the model were determined by trial and error. Regarding  $\sigma_0$  and  $\sigma_1$ , methods to identify them have been proposed [11, 12] but those methods utilize some approximation that holds in the presliding regime. It is difficult for a hydraulic actuator to be operated in the presliding regime and, therefore, the methods proposed so far cannot be applied to hydraulic actuators. In addition, for the modified LuGre model, a new parameter, the time constant,  $\tau_h$ , is added. Some method to identify those parameters needs to be developed.

In this paper, a method to identify the dynamic parameters is proposed. In addition, the effect of the supply pressure on the dynamic parameters is examined.

## EXPERIMENTAL APPARATUS AND METHOD

Figure 1 shows a schema of the experimental apparatus used. A single rod hydraulic cylinder, of which stroke, internal diameter and piston rod diameter are 0.2m, 0.032m and 0.018m, respectively, is used. The hydraulic cylinder is fixed horizontally on a surface plate. Sinusoidal or step signals are supplied to the servo amplifier through a 12 bit digital-to-analogue (D/A) converter and then the velocity of the hydraulic piston is varied almost sinusoidally or reaches a constant value corresponding to the input to the servo amplifier. The pressures,  $p_1$ ,  $p_2$ , in the cylinder chambers and the acceleration,  $a$ , of the piston are measured using pressure transducers and an accelerometer, respectively and are read into the computer through amplifiers and a 12 bit analogue-to-digital (A/D) converter. The piston velocity is measured using a tachogenerator by converting a linear motion of the piston to a rotational motion through a ball-screw (not shown in Fig.1). The friction force is obtained based on the equation of motion of the hydraulic piston as follows:

$$F_r = p_1 A_1 - p_2 A_2 - ma \quad (1)$$

Steady-state friction characteristics are obtained by supplying stepwise inputs with different magnitudes to the servo valve and by measuring the steady values of the pressures and velocity. In order to examine the effect of pressure on the friction characteristics, experiments are made at the supply pressures of 3, 5 and 7 MPa. The oil temperature was kept at  $303 \pm 2$  K.

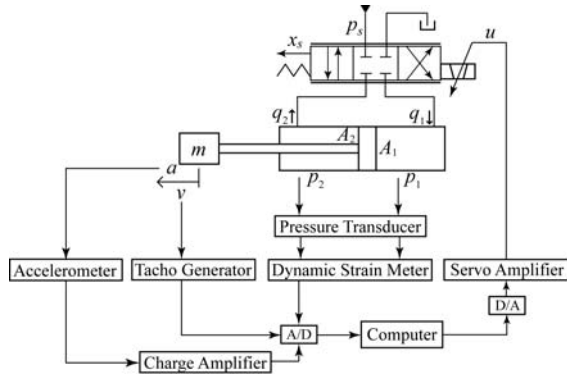


Figure 1 Schema of experimental apparatus

### MODIFIED LUGRE MODEL

The Stribeck function,  $g$ , was modified by incorporating a dimensionless lubricant film thickness parameter,  $h$ . The modified LuGre model is given below.

i) Equations corresponding to the LuGre model

$$\frac{dz}{dt} = v - \frac{\sigma_0 z}{g(v, h)} v \quad (2)$$

$$g(v, h) = F_c + [(1-h)F_s - F_c] e^{-(v/v_s)^n} \quad (3)$$

$$F_r = \sigma_0 z + \sigma_1 \frac{dz}{dt} + \sigma_2 v \quad (4)$$

ii) Lubricant film dynamics

$$\frac{dh}{dt} = \frac{1}{\tau_h} (h_{ss} - h) \quad (5)$$

$$\tau_h = \begin{cases} \tau_{hp} & (v \neq 0, h \leq h_{ss}) \\ \tau_{hm} & (v \neq 0, h > h_{ss}) \\ \tau_{h0} & (v = 0) \end{cases} \quad (6)$$

$$h_{ss} = K_f |v|^{2/3} \quad (|v| \leq |v_b|) \quad (7)$$

$$K_f = (1 - F_c/F_s) |v_b|^{-2/3} \quad (8)$$

iii) Steady-state friction characteristic

$$F_{rss} = F_c + [(1 - h_{ss})F_s - F_c] e^{-(v/v_s)^n} + \sigma_2 v \quad (9)$$

In the LuGre model, the absolute value of the velocity is usually used in the second term in Eq.(2). However, when assigning negative values to  $F_c$ ,  $F_s$  and  $v_s$  for negative velocity range, the symbol of the absolute

value is not necessary. Letting  $h$  in Eq.(3) and  $h_{ss}$  in Eq.(9) be null leads to the LuGre model. The time constant shown by Eq.(6) usually takes the relation,  $\tau_{hp} < \tau_{hm} < \tau_{h0}$ .

All the parameters, except for  $\sigma_0, \sigma_1, \tau_h$ , included in Eqs.(2) to (9) can be determined from measured steady-state friction characteristics by using the least-squares method. However, the above three parameters were determined by trial and error in [10].

### PARAMETER IDENTIFICATION

#### Identification of time constant, $\tau_h$

In this section, methods to identify the time constant of the lubricant film dynamics are described first. The value of the second term in Eq.(4) becomes almost null except for immediately after the start from rest and for immediately after velocity reversal. Therefore, except for immediately after start and velocity reversal, the relation,  $F_r = g(v, h) + \sigma_2 v$ , holds and the following equation is derived:

$$h = 1 - \frac{F_r - F_c + F_c e^{-(v/v_s)^n} - \sigma_2 v}{F_s e^{-(v/v_s)^n}} \quad (10)$$

If the values of the friction force,  $F_r$ , and velocity,  $v$ , can be obtained in real time, the variation of the lubricant film thickness parameter,  $h$ , is calculated from Eq.(10). When the velocity is increased or decreased stepwise from a certain velocity, the film thickness parameter,  $h$ , is expected to be varied approximately exponentially. The time constants,  $\tau_{hp}$  and  $\tau_{hm}$  can be obtained by curve-fitting a calculated variation of  $h$  with time using an exponential function.

During dwell period, lubricant film thickness is decreased with time. The break-away force (maximum friction force observed immediately after start) observed at the subsequent start is expected to be larger when the dwell time is longer. Equation (11) is obtained by substituting  $v = 0$  into Eq.(10) and holds only for dwell period. However, assuming that Eq.(11) approximately holds also at start after dwell period and substituting the observed break-away force into  $F_r$  of Eq.(11), the calculated film thickness can be regarded as the film thickness immediately before the start.

$$h = 1 - \frac{F_r}{F_s} \quad (11)$$

The time constant,  $\tau_{h0}$ , for the dwell period can be identified by plotting the break-away force against the dwell time before the start.

#### Identification of $\sigma_0$ and $\sigma_1$

The stiffness,  $\sigma_0$ , of the bristles strongly affects the

magnitude and rise time of the break-away force. A larger  $\sigma_0$  yields a larger break-away force and a shorter rise time. The value of  $\sigma_0$  can be identified by comparing the magnitude and rise time of the break-away force estimated by an observer with those obtained by simulation. The value of  $\sigma_1$  can be determined by using the relation  $\sigma_1 = \sqrt{\sigma_0}$  [6].

### Observer for friction force and velocity

The friction force is obtained from Eq.(1). In order to measure unsteady-state friction force accurately, it is necessary to measure the pressures, acceleration and velocity. However, for the purpose of the identification of the parameters included in the modified LuGre model, the accelerometer and tachogenerator are not necessarily needed. The friction force and velocity can be estimated by an observer. A Luenberger type observer can be given by

$$\frac{d}{dt} \begin{bmatrix} \hat{x}_p \\ \hat{v} \\ \hat{F}_r \end{bmatrix} = \begin{bmatrix} 0 & 1 & 0 \\ 0 & 0 & -\frac{1}{m} \\ 0 & 0 & 0 \end{bmatrix} \begin{bmatrix} \hat{x}_p \\ \hat{v} \\ \hat{F}_r \end{bmatrix} + \begin{bmatrix} 0 \\ \frac{1}{m} \\ 0 \end{bmatrix} (A_1 p_1 - A_2 p_2) + \mathbf{f}(x_p - \hat{x}_p) \quad (12)$$

In practice, Eq.(12) is discretized.

## RESULTS AND DISCUSSION

Figure 2 shows the steady-state friction characteristics measured at the supply pressures of 3, 5 and 7 MPa. Positive velocity corresponds to the extending stroke of the piston and negative one to the retracting stroke. The friction force is increased with increasing supply pressure in the extending stroke ( $v > 0$ ) but is not varied so much in the retracting stroke ( $v < 0$ ). The static parameters, the parameters that describe the steady-state friction characteristics, were determined by the least-squares method.

Figure 3 compares the measured piston velocity and friction force with the ones estimated by the observer, Eq.(12). As can be seen from Fig.3, the velocity and friction force are accurately estimated by the observer. The maximum friction force is observed immediately after the start of the motion and is called the break-away force. Maximum forces observed at and after the second cycle become smaller than the break-away force, as shown in Fig.3(b), because lubricant films are formed between sliding surfaces, which are mainly the piston packing/cylinder inner wall and the rod packing/piston rod.

Figure 4 shows an example of the dimensionless film thickness obtained when the piston velocity was

increased stepwise from rest to 0.016 m/s. As shown in Fig.4, the film thickness is increased with time and its variation can well be approximated by a first-order lag element, i.e., by Eq.(5). For the case of Fig.4, the time constant was identified as  $\tau_{hp}=0.29$  s.

An example of the variation of the film thickness under a stepwise decrease (from 0.015 to 0.003 m/s at  $t=3$  s) in the velocity is shown in Fig.5. The film thickness is decreased significantly slowly compared with the case of velocity increase (Fig.4). By curve-fitting, the time constant was identified as  $\tau_{hm}=2.0$  s for Fig.5.

Such experiments as Figs.4 and 5 were done under various velocities and the time constants were identified in a similar way.

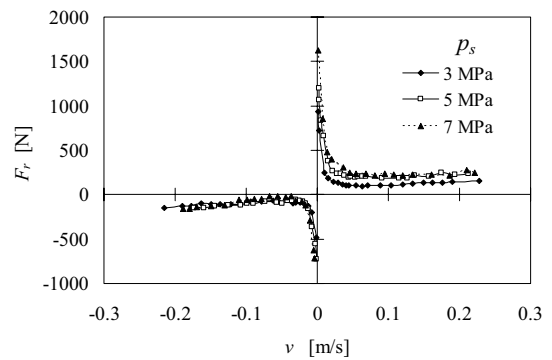
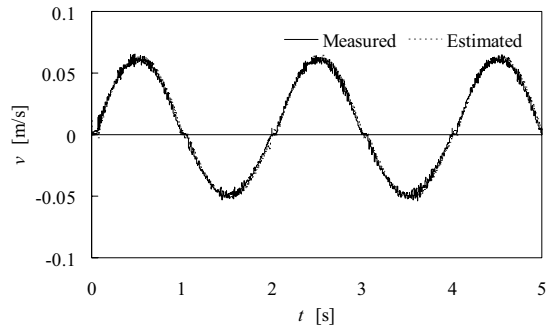
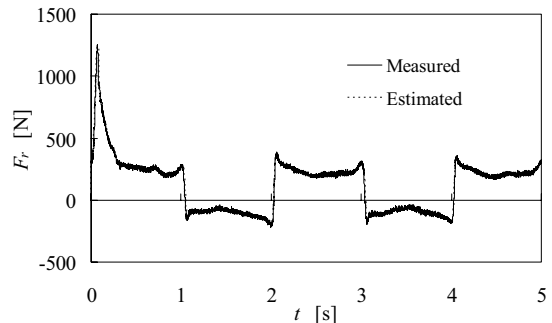


Figure 2 Steady-state friction characteristics



(a) Variation of piston velocity



(b) Variation of friction force

Figure 3 Comparison of measured velocity and friction force with estimated ones ( $p_s=5$ MPa)

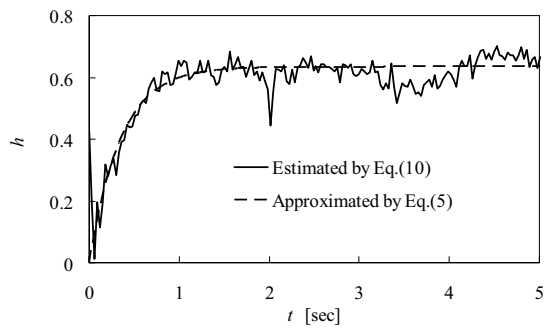


Figure 4 Example of lubricant film thickness variation under stepwise increase in velocity ( $v=0$  to  $0.016$  m/s,  $p_s=5$ MPa)

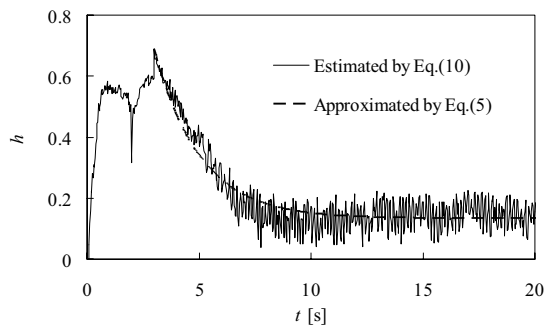


Figure 5 Example of lubricant film thickness variation under stepwise decrease in velocity ( $v=0.015$  to  $0.003$  m/s,  $p_s=5$ MPa)

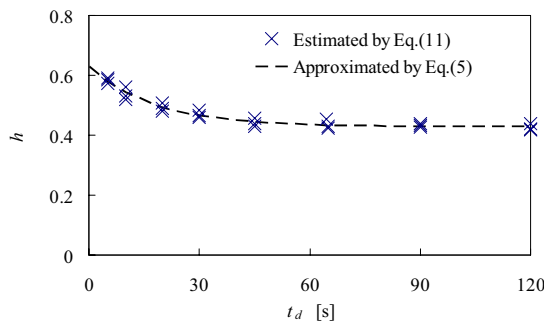


Figure 6 Film thickness variation during dwell period ( $p_s=5$ MPa)

Figure 6 shows the relation between the dwell time and the lubricant film thickness estimated by Eq.(11), into which measured break-away forces observed at starting after different dwell times are substituted. The break-away force was increased with the increase in the dwell time before starting and was saturated to a constant value. Therefore, the relation shown in Fig.6 was obtained. Curve-fitting brings a time constant of 17 s for dwell period for the case of Fig.6.

Experiments were conducted at different supply pressures and the average time constants were obtained as shown in Table 1. All the time constants for

accelerating, decelerating, and dwell periods are increased with increasing supply pressure. This indicates that the oil is to some degree hard to be taken into and to be squeezed out from the sliding surfaces at higher pressures.

Table 1 Time constants at different supply pressures

$p_s$ [MPa]	$\tau_{hp}$ [s]	$\tau_{hm}$ [s]	$\tau_{h0}$ [s]
3	0.13	1.1	8.1
5	0.28	1.8	17
7	0.32	2.4	43

The stiffness of the bristles was determined by comparing the break-away force and its rise time estimated by the observer with simulated ones. The simulation was done using MATLAB/Simulink and measured velocity wave forms were used as the input to the modified LuGre model. Experiments done under various conditions showed that the value of  $\sigma_0=10^8$  N/m is most appropriate and is not dependent on the supply pressure for the hydraulic cylinder used. The value of  $\sigma_1$  was determined as the square root of  $\sigma_0$ , i.e.,  $\sigma_1=10^4$  Ns/m.

Figures 7 and 8 show the comparison between measured unsteady-state friction characteristics and simulated ones using the modified LuGre model, in which the identified dynamic parameters as well as the static parameters (not shown) were used. The simulation predicts larger friction force immediately before stop than the experiment (Fig.8). However, comparisons under various conditions including Figs.7 and 8 showed that the simulation results agree relatively well with the measured results. This indicates the proposed method to identify the dynamic parameters is appropriate.

## CONCLUSION

In this investigation, a method to identify the dynamic parameters of the modified LuGre model was proposed and was applied to a hydraulic cylinder. In addition, the effect of the supply pressure on the unsteady-state friction characteristics was examined. Simulation results agreed relatively well with measured results. It has been demonstrated that the proposed identification method is appropriate. In addition, it has been shown that the time constant of the lubricant film dynamics is increased with increasing supply pressure and that the stiffness of bristles does not depend on the supply pressure.

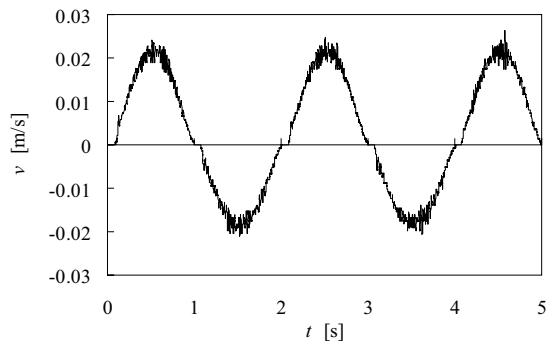
## REFERENCES

1. Armstrong-Helouvry B. Control of machines with friction, Kluwer Academic Publishers, 1991.
2. Armstrong-Helouvry B, Dupont P, Canudas de Wit C. A survey of models, analysis tools and compensation

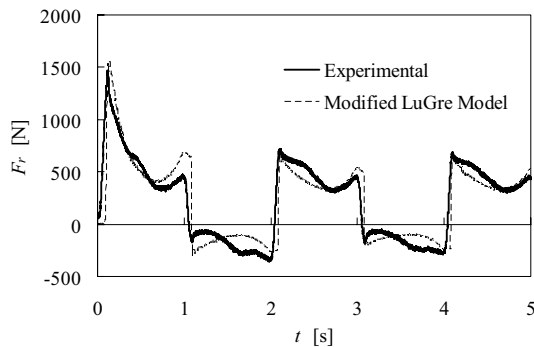
methods for the control of machines with friction, *Automatica*, 1994, **30**-7, pp.1083-1138.

3. Hibi A, Ichikawa T. Mathematical model of the torque characteristics for hydraulic motors, *Bull. JSME*, 1977, **20**-143, pp.616-621.
4. Yanada H, Inaba T, Ichikawa T. Experimental approach to unsteady friction characteristics of a hydraulic motor in low-speed range, *Trans. Japan Soc. Mech. Eng. (Ser. B)*, 1990, **56**-528, pp.2430-2437. (in Japanese)
5. Haessig D A Jr, Friedland B. On the modeling of friction and simulation, *J Dynamic Systems, Measurement and Control*, 1991, **113**-3, pp.354-362.
6. Canudas de Wit C, Olsson H, Åström, K J, Linschinsky P. A new model for control of systems with friction, *IEEE Trans Automatic Control*, 1995, **40**-3, pp.419-425.
7. Dupont P E, Dunlop E P. Friction modeling and PD compensation at very low velocities, *J Dynamic Systems, Measurement and Control*, 1995, **117**-1, 8-14.
8. Swevers J, Al-Bencer F, Ganseman C G, Prajogo T. An integrated friction model structure with improved presliding behavior for accurate friction compensation, *IEEE Trans Automatic Control*, 2000, **45**-4, pp.675-686.

9. Dupont P, Hayward V, Armstrong B, Altpeter F. Single state elastoplastic friction models, *IEEE Trans Automatic Control*, 2002, **47**-5, pp.787-792.
10. Yanada H, Sekikawa Y, Modeling of dynamic behaviors of friction, *Mechatronics*, 2008, (in press)
11. Hensen R H A, van de Molengraft M J G, Steinbuch M, Frequency domain identification of dynamic friction model parameters, *IEEE Trans. Contr. Syst. Tech.*, 2002, **10**-2, pp.191-196.
12. Madi M S, Khayati K, Bigras P, Parameter estimation for the LuGre friction model using interval analysis and set inversion, *IEEE Int. Conf. Syst. Man Cybernetics*, 2004, pp.428-433.

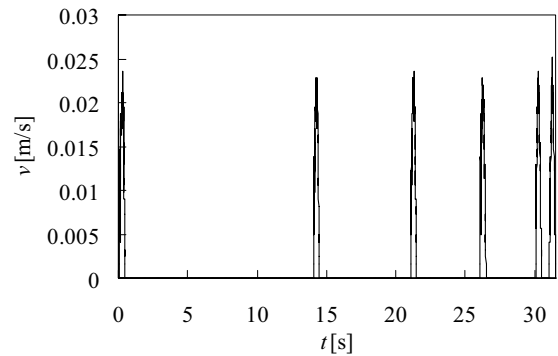


(a) Velocity variation

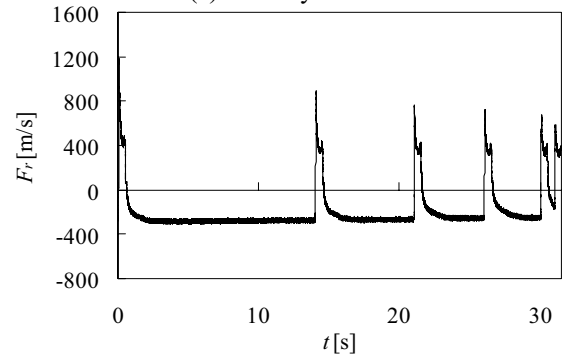


(b) Variation of friction force

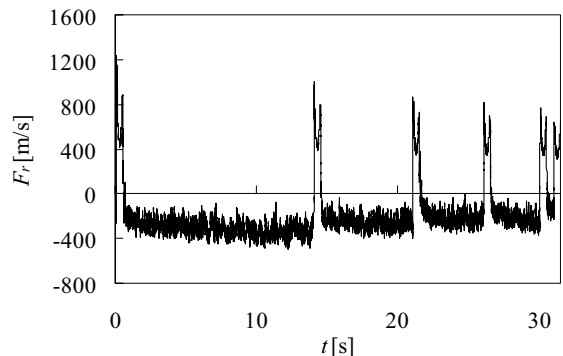
Figure7 Comparison between measured and simulated friction force (without dwell period,  $p_s=7$  MPa)



(a) Velocity variation



(b) Measured friction force



(c) Simulation using modified LuGre model

Figure 8 Comparison between measured and simulated friction force (with dwell period,  $p_s=7$  MPa)